Ion beam mixing by focused ion beam

Árpád Barna, László Kotis, János L. Lábár, Zoltán Osváth, Attila L. Tóth, and Miklós Menyhárd[a)]
Research Institute for Technical Physics and Materials Science, Budapest H-1525 P. O. Box 49, Hungary

Anton Zalar and Peter Panjan
Jožef Stefan Institute, Jamova 39, 1000 Ljubljana, Slovenia

(Received 14 June 2007; accepted 16 July 2007; published online 12 September 2007)

Si amorphous (41 nm)/Cr polycrystalline (46 nm) multilayer structure was irradiated by 30 keV Ga^+ ions with fluences in the range of 25–820 ions/nm^2 using a focused ion beam. The effect of irradiation on the concentration distribution was studied by Auger electron spectroscopy depth profiling, cross-sectional transmission electron microscopy, and atomic force microscopy. The ion irradiation did not result in roughening on the free surface. On the other hand, the Ga^+ irradiation produced a strongly mixed region around the first Si/Cr interface. The thickness of mixed region depends on the Ga^+ fluence and it is joined to the pure Cr matrix with an unusual sharp interface. With increasing fluence the width of the mixed region increases but the interface between the mixed layer and pure Cr remains sharp. TRIDYN simulation failed to reproduce this behavior. Assuming that the Ga^+ irradiation induces asymmetric mixing, that is during the mixing process the Cr can enter the Si layer, but the Si cannot enter the Cr layer, the experimental findings can qualitatively be explained. © *2007 American Institute of Physics*. [DOI: 10.1063/1.2776009]

I. INTRODUCTION

During ion bombardment large energy dissipation occurs in the irradiated material, which causes alterations. One of the several simultaneously occurring processes is the ion beam mixing (or shortly ion mixing), which means the mixing of initially separated layers, clusters, etc. Ion mixing can produce equilibrium and nonequilibrium atomic arrangements as well. The latter, on the other hand, might exhibit exotic and sometimes desired properties. High energy [some hundreds of kilo-electron-volts (keV)] ion mixing experiments have really proved that equilibrium as well as nonequilibrium mixtures can be produced at a depth determined by the average penetration depth (projected range) of the projectile.[1] In the case of a bilayer system originally separated by sharp interface the concentration distribution formed due to the ion mixing is usually an error function, since the atomic movements during ion mixing are similar to those occurring in usual diffusion.[2] This reasoning is more or less independent on the type of projectile, its energy, etc. Recently, we have shown that the mixing efficiency in case of Cu/Co system is the same at 1 and 400 keV.[3]

Changing the energy of the projectile we can tune the depth of the mixed region, which might be advantageous for various applications; e.g., in the case of some tens of keV ion energy the typical projected range is about 10 nm, which might be interesting from a nanotechnology point of view. This energy range is easily available since the focused ion beam (FIB) guns operate in this range.

FIB is widely used tool for nano or/and microtechnology like ion milling [making specimens for transmission electron microscopy (TEM)], high dose writing implantation, ion mixing, etc.[4] These important applications are possible due to the high density energy dissipation occurring in FIB exposure, which causes serious alteration of the irradiated volume. To mention only a few from the many applications we refer to the work of McGrouthera *et al.*,[5] who studied the change of crystalline structure due to FIB irradiation, which affected the magnetic properties. Akhmadaliev *et al.*[6] produced nanowire by FIB synthesis of Co and Si, while Gonzalez *et al.*[7] used FIB to repair interconnects. Gazzadi *et al.*[8] used FIB for fabrication of a nanogap electrode, etc.

Despite the great many applications of FIB there are only a few studies which deal with the physical processes occurring in the material during FIB exposure; e.g., Bischoff *et al.* applied FIB on SiC using various projectiles in the energy range of 35–70 keV and determined the sputtering yields and swelling in steady state condition.[9] The experimental results agreed well with those derived from simulations. Park *et al.*[10] studied the Ga implantation profile in lateral and depth direction in magnetic material by applying Auger electron spectroscopy (AES) depth profiling. The experimentally measured depth profile poorly agreed with that provided by simulation. Gazzadi *et al.* while fabricating a nanoelectrode by FIB (Ref. 8) measured the Ga depth profile applying AES depth profiling and found good agreement and strong deviation with respect tothe simulation in the case of the usual and iodine assisted Ga irradiation, respectively. Boxleitner *et al.*[11] developed a simulation devoted to the calculation of the FIB induced damage (in pure material amorphization) and morphology change. They applied it to bulk Si and received good agreement with TEM studies.

We do not know, however, any work reporting on measurement of ion mixing, that is, the mixing occurring at the interface of two pure materials due FIB irradiation. In this work we report on AES depth profiling, cross-sectional TEM (XTEM) and atomic force microscopy (AFM) studies ap-

[a)]Electronic mail: menyhard@mfa.kfki.hu

plied on Si/Cr multilayer sample irradiated by Ga ions of energy 30 keV using fluences in the range of 25 -820 ions/nm^2. It turned out that "strange" ion mixing occurs in the whole fluence range. The affected region contains a strongly mixed region, which joins to underlying layer with a sharp interface. The concentration distribution produced by Ga^+ irradiation cannot be approximated by an error function, and it cannot be described by transport of ions in matter (TRIM) simulation. On the other hand, assuming asymmetric mixing qualitative explanation of the experiments is possible.

II. EXPERIMENT

A. Sample and characterization

The Si/Cr multilayer was sputter deposited on silicon (111) substrates. The thickness of the individual layers was controlled using a quartz crystal microbalance during sputter deposition.

XTEM images were taken by a Philips CM20 200 kV analytical microscope and were used (a) to determine the actual thickness of the individual layers, and intrinsic interface roughness prior Ga^+ irradiation and (b) to characterize the layer structure after Ga^+ irradiation.

The sample preparation method for XTEM, which is described in details by Barna *et al.*,[12] consisted of a mechanical thinning and polishing to a thickness of 50 μm, and of grazing incidence (88° with respect to the surface normal) ion beam thinning with 10 kV Ar^+ ions. The ion beam thinning was finished with 3 keV Ar^+ bombardment.

B. FIB irradiation

The samples were irradiated using the Canion FIB optics of a LEO 1540XB [FEG scanning electron microscopy (SEM)-FIB] cross beam system. The 200×200 μm^2 area to be mixed had been located using the SEM secondary electron image (SEI), then checked on a single pass FIB SEI image. The size of the area as well as the energy (30 keV), intensity (5.5 nA), and angle of incidence (5° with respect to the surface normal) of the Ga^+ ion beam were kept constant in the experiment. The dose was varied by changing the time of single pass irradiation (40–1280 s) controlled by the FIB etching module of the software. The corresponding fluences were in the range of $25-820$ ions/nm^2.

C. AFM studies

The AFM measurements were done in tapping mode using a Nanoscope IIIa operating in air. The root-mean-square (rms) roughness of the irradiated and for reference purpose the nonirradiated areas were measured on a 500×500 nm^2 areas. The surface recession was determined from line scans running from the nonirradiated area into the crater. The distance of the average surface from the bottom of the crater was taken as a measure of the geometrical recession.

D. AES depth profiling

The AES depth profiling was carried out in our dedicated systems.[13] 1 keV Ar^+ was used for ion bombardment with angle of incidence of 82° (with respect to the surface normal). The ion current was kept constant during the sputtering. The sample was rotated (4 rev/min) during ion bombardment to reduce the surface morphology development. The AES spectra were recorded by a STAIB DESA 100 preretarded cylindrical mirror analyzer in direct current mode. The primary electron current was 30 nA with a diameter of about 40 μm. The measured emitted current curves were numerically differentiated and the peak-to-peak amplitudes were used as a measure of the amount of material present. The concentrations were calculated from the peak-to-peak amplitudes by applying the relative sensitivity factor method.[14] The relative sensitivity factors for Si and Cr were determined by internal standards (measured on the pure regions of the sample). Ga data given by Ref. 14 were used.

E. Evaluation of the removed layer thickness

In AES depth profiling the sputtering time is measured. Its conversion to sputtered depth is not trivial if the density and the sputtering yield of the materials involved are strongly different. In the present case the atomic densities are strongly different being 49.7 and 83.3 at/nm^3 for Si and Cr, respectively. Luckily the relative sputtering yield, Y_{Cr}/Y_{Si}, for the sputtering conditions used, 1 keV $Ar^+/82°$ are rather similar being around 0.7 (Ref. 15), thus this correction is not so serious. To convert the sputtering time to removed depth we have followed the same procedure, which has been published earlier[15] and here it is only shortly summarized.

First, we suppose that the mixture is an ideal solution, and thus the average density (ρ) of the mixture can be calculated as $1/\rho=\Sigma(X_i/\rho_i)$ where ρ_i is the density of pure component i, and X_i is the atomic concentration.

Second, we have to determine the sputtering yields. This is not easy task since experimental sputtering yield data for pure materials for the sputtering conditions we have applied are not known. Moreover, it is well known that even if the data for pure materials are known the sputtering yield of the alloys, mixture, etc., cannot be always easily derived from them.[16] Thus our only possibility is to estimate the necessary sputtering yield values by the help of available simulations. Applying SRIM simulation[17] we can calculate the total (Y) and partial sputtering yields (Y_i) as a function of the composition for any ion bombardment conditions. According to those simulations in this case the simple expression of $Y=\Sigma X_i Y_i^o$ gives the total sputtering yield in the whole concentration range with a accuracy of 15%, where Y_i^o is the sputtering yield of the pure element i. The partial sputtering yield, on the other hand, can be approximated as X_iY, with similar accuracy.

F. The representation of AES depth profile

The AES depth profile is generally given as atomic concentration versus depth. This is a good representation if the density of the material does not vary strongly since the integral of this curve multiplied by the density gives the removed numbers of atoms per unit area. If the density strongly changes along the depth, the usage of this representation is misleading (the integral multiplied the effective lat-

TABLE I. The surface roughness (rms in nm) and recession (nm) as a function of fluence of Ga^+(30 keV/5°) irradiation measured by AFM. In the second column the roughness measured on the nonirradiated area (close to the irradiated region) is also shown for reference purpose. The roughness was measured on an area of 500×500 nm^2.

Fluence density (ions/nm^2)	Roughness reference (nm)	Roughness irradiated (nm)	Recession (nm)
25	0.3	0.2	0.5±0.2
51	0.3	0.17	1±0.2
205	0.3	0.21	4±1
410	0.35	0.7	6±1
820	0.35	0.19	10.5±1

tice constant does not give the number of removed atoms). To cope with this problem we will use the number of atoms in unit area (instead of the atomic concentration) versus depth curve.

G. Simulation of FIB damage and restoration of the true depth profile

The dynamic TRIM (TRIDYN) code of Moller's *et al.*[18] has been applied to simulate the effect of the Ga^+ irradiation. The concentration distributions for all irradiation experiments were calculated using this code and will be compared with the derived true profiles. For TRIDYN simulation the default input parameters (offered by the code) but one were used as follows: bulk binding energies 0 eV for all elements, surface binding energies 4.8, 4.2, and 2.8 eV for Si, Cr, and Ga, respectively. The cutoff energy for Si was chosen, however, to be 2.1 eV.

The same code with the same parameters was used to restore the true depth profile from the measured depth profile (see discussion).

III. RESULTS

The irradiated area, 200×200 μm^2, could be easily seen by naked eyes as well, which helped the positioning of the various measurements.

According to the XTEM studies the structure of the sample was as follows: Si1 41nm/Cr1 46nm/Si2 41nm/ Cr2 46nm/ Si3 42nm/ Cr3 53nm. The layers are numbered starting from the free surface. The structure of the Cr layers is polycrystalline with a typical grain size of 15 nm, while the Si layers are amorphous. The intrinsic values of the interface roughness were found to be 1–2 nm.

The rms roughness values of the irradiated areas have been measured by AFM on a 500×500 nm^2 area as well as the surface recession as a function of fluence. For reference purpose we also measured the surface roughness on the nonirradiated areas close to the irradiated ones. All AFM data are summarized in Table I.

Figure 1 shows the as measured AES depth profiles (1 keV/82°, Ar^+, rotated specimen) of samples without (0) and with (the highest) Ga^+, 30 keV/5° 820 ions/nm^2 irradiation. It is clear that irradiation affects only the first Si1 and Cr1 layers; the Cr1/Si2 interface is unaffected, however. Thus in the following we will deal only beginning part of the

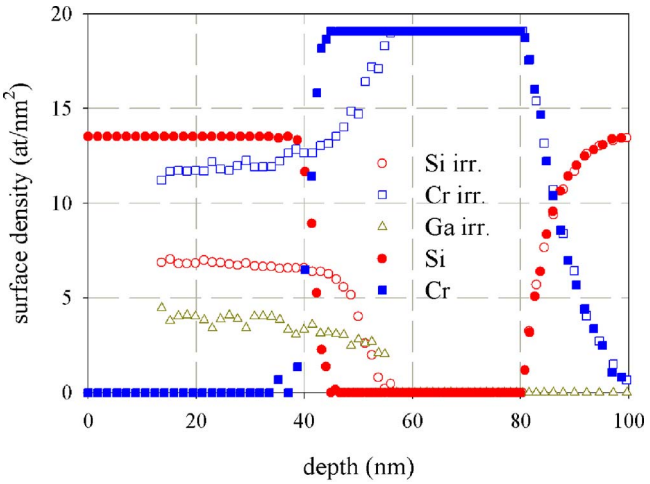

FIG. 1. (Color online) Si, Cr, and Ga AES depth profiles of samples without (0 ions/nm^2) full symbols, and with Ga^+ irradiation (820 ions/nm^2) open symbols. The second, Cr1/Si2, Si transitions of the two samples are fitted to the same, 83.5 nm, depth. Note that the shapes of the two interfaces are the same within the experimental error.

depth profile, up to about 50 nm, which completely involves the irradiation affected region. To be able to compare the depth profiles of variously irradiated samples the reference frame will be fixed to the substrate. This can be done by fitting the depth profiles at the Cr1/Si2 interface (which is unaffected by the irradiations we used). In this representation only the profile without irradiation starts at 0, all the others starts at some positive value (the missing part is the removed layer thickness). The removed layer thickness derived in the AES depth profiling is compared with those provided by AFM and XTEM; reasonable agreement was found. In Fig. 2(a) we show the as measured Si depth profiles recorded on samples irradiated by applying fluences of 0, 25, 51, 205, 410, and 820 ions/nm^2, while in Fig. 2(b) the enlarged version of the profiles recorded at fluences of 0, 25, and 51 ions/nm^2 are shown. It is clear that the Ga irradiation even at the lowest fluence, 25 ions/nm^2, strongly affects the concentration distribution across the interface; the length of the transition region (depth resolution) is more than double than that without irradiation. Increasing the fluence, a characteristic shape of the concentration distribution forms. It can be characterized by three different slopes, where the middle, being in the interface region, has the lowest slope. Thus the ion mixing in this region is the highest. This feature is amplified with larger fluences reaching the nearly constant (along the depth) concentration distribution at 820 ions/nm^2 fluence. "Normal ion beam mixing" produces a more or less error function type of concentration distribution. In the present case this is evidently not true.

IV. DISCUSSION

The depth resolution of the AES depth profiling among others depends on the intrinsic (free surface roughness) and the sputtering induced roughening.[19–23] Applying specimen rotation during ion bombardment[23] and grazing angle of incidence[20,21] minimize the sputtering induced roughening; this is why we applied specimen rotation and angle of inci-

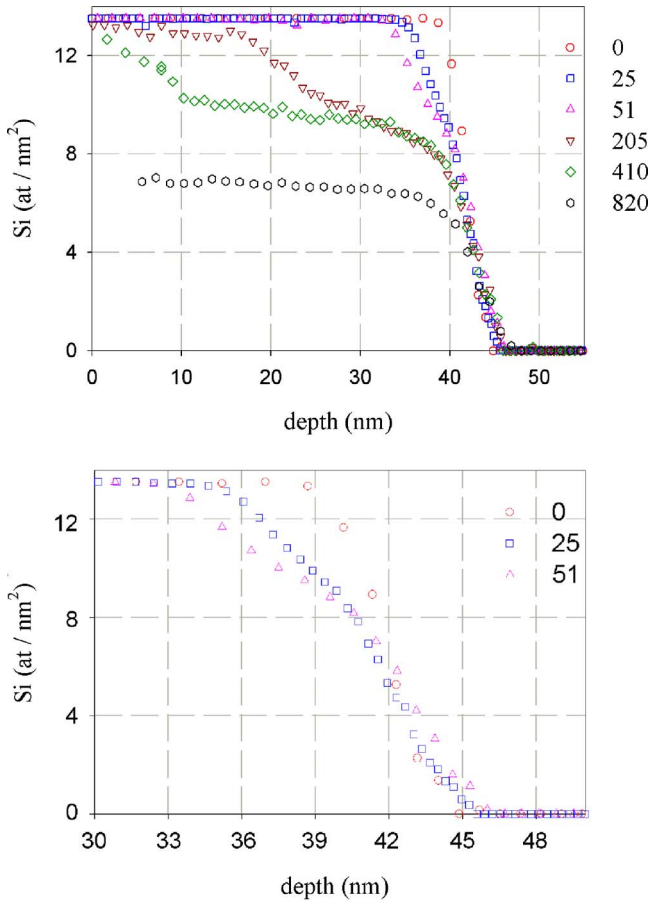

FIG. 2. (Color online) (a) The as measured Si AES depth profiles. The curves are fitted to the position of the Cr1/Si2 interface. The parameters shown in the figure are the fluences (ions/nm^2). (b) The enlarged part of (a).

dence of 82° (with respect to the surface normal). Moreover, according to the AFM measurement smoothening took place on the free surface (except for irradiation with 410 ions/nm^2, where slight roughening was observed) due to the Ga^+ ion irradiation, instead of an expected surface roughening. Adams *et al.* reported similar finding for carbon.[24] The phenomenon can be explained by an ion-enhanced transport process.[25] Even in the case of the irradiation with 410 ions/nm^2 the roughening of the free surface is rather modest, 0.7 nm, less than the intrinsic interface roughness. Thus we might hope that the intrinsic and sputtering induced roughening does not affect our results. This assumption will be justified later by considering the evaluation of the experimental results. Thus in the following discussion we will ignore the free surface and irradiation induced roughening.

Based on the as measured depth profiles, shown in Figs. 2(a) and 2(b), we can make some simple statements as follows:

(a) independently from the fluences there is a middle region on all depth profiles (except irradiation of 25 ions/nm^2), where the slope of the Si depth profile is the lowest;
(b) independently from the fluence the last parts of the Si depth profiles (connecting the mixed region to the pure Cr) are similar; and
(c) the slopes of the beginning part of the Si depth profiles (from the free surface), if exist, are always lower than those of the last parts.

At this point it should be emphasized that the as measured AES depth profile is a difficult transformation of the concentration distribution initially (before the AES depth profiling) present in the sample, which will be called as true depth profile. Thus before the actual discussion we should deal with derivation of the true depth profile.

A. Calculation of the true depth profile

In AES depth profiling thin layers are removed sequentially by ion bombardment, and the newly formed surface is analyzed. The material removal process alters the surface close regions by means of ion mixing, ion bombardment induced roughening, etc. The projected range of the Ar^+ ions for 1 keV/82° bombardment is 1.5±1 nm, thus we expect ion induced changes in this thickness range. The AES analysis because of the finite escape depth of the Auger electrons provides an average composition. In the present case since the inelastic mean free paths (IMFP) of the measured Auger electrons are 0.51 and 1.09 nm, for Si and Cr,[26] respectively the composition is averaged for a 1–1.5 nm thick surface region. If the true profile can be considered as quasiconstant for such length scales, 2–3 nm, then the earlier effects can be easily corrected and the as measured AES depth profile is similar to the true depth profile. On the other hand, if the concentration strongly changes within this length scale, e.g., there is a step function transition, then the as measured AES depth profile considerably different from the true profile and the derivation of the true profile is necessary. According to Fig. 2 the transition to the pure Cr layer is rather sharp thus the derivation of the true profile in this region should be carried out.

For the derivation of the true profile we apply our trial-and-error method.[27] It's essence is the following. First, an initial concentration distribution is assumed, which is in fact the trial true depth profile. After we simulate the AES depth profiling procedure, that is, we apply sequential ion bombardment and measurement of Auger intensities. The ion bombardment is simulated by the dynamic TRIDYN code of Moller *et al.*,[18] while the AES intensities are calculated from the concentration distribution provided TRIDYN code. To get the Auger intensities we used the earlier IMFP values. The ion bombardment is applied as long as the desired layer thickness is removed. This procedure provides the simulated AES depth profile, which can be compared with the measured one. The initial concentration distribution is varied until the simulated and measured AES depth profiles agree. The initial surface roughness can also be involved in the calculation. The calculation cannot account for bombardment induced roughening, but as we have seen the probability of this process is low.

We can check our procedure in case of the nonirradiated sample, where the initial concentration distribution, the true depth profile, is known from the TEM image; it is a step function transition, with an intrinsic interface roughness of

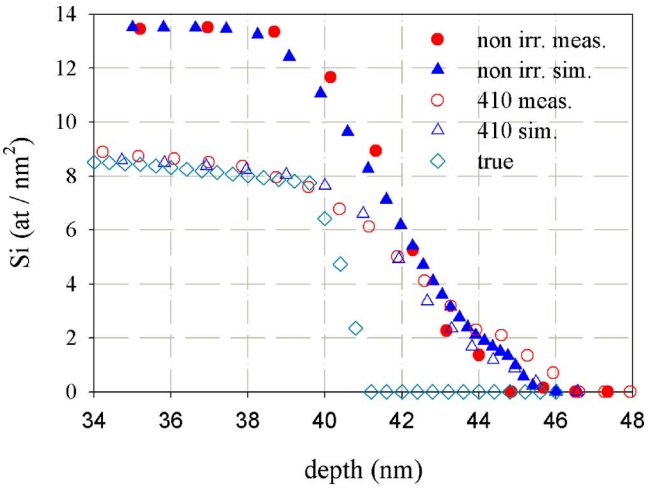

FIG. 3. (Color online) The as measured Si AES depth profiles of the nonirradiated sample (nonirraditaed measured) full symbols, and irradiated by 410 ions/nm^2 (410 meassured) open symbols, and the corresponding simulated depth profiles, and the true profile of the irradiated sample in the region of the first Si1/Cr1 interface. The true profile of the nonirradiated sample (not shown in the figure) is a step function.

about 1.5 nm. Using the initial conditions and numbers from earlier the simulated depth profile agrees well with the measured one as it is shown in Fig. 3.

Interestingly enough all as measured AES depth profiles follow the same slope where the mixed layer is joined to the pure Cr. This also means that the transition between the mixed region and the pure Cr is the same, step function like, independently from the fluence applied. To support this statement we derived the true depth profile from as measured AES depth profile corresponding to irradiation of 410 ions/nm^2. In Fig. 3 we show the true depth profileand the measured and simulated depth profiles. Since the agreement between the simulated and measured depth profiles is reasonable good, we accept the true depth profile. The true depth profile again shows a step function type of transition between the strongly mixed region and the pure Cr. Figure 3 also demonstrates that in the mixed region (which slowly varying function within a 2–3 nm length scale) the true depth profile coincides with the measured one as it is expected. For comparison in Fig. 3 we also show the measured and simulated depth profiles of the nonirradiated sample.

In case of the samples irradiated with fluences of 25 and 51 ions/nm^2 there are steps in the Si AES depth profiles around 40 nm depth [Fig. 2(b)]. These features are also candidate for reconstruction but our method, because of the small changes, provides the true depth profiles with rather large uncertainties thus it has not been applied.

Based on the earlier, we conclude that the concentration distribution produced by the Ga^+ irradiation is rather strange one. We can define a strongly mixed region around the original interface. The thickness of this region increases with increasing Ga^+ fluence. This strongly mixed region is connected to the free surface by a much weaker mixed region, while its connection to the pure Cr seems to be abrupt. This is a rather unusual behavior thus we looked for an independent verification. Figures 4(a) and 4(b) show the XTEM images taken from irradiated region of the samples irradiated

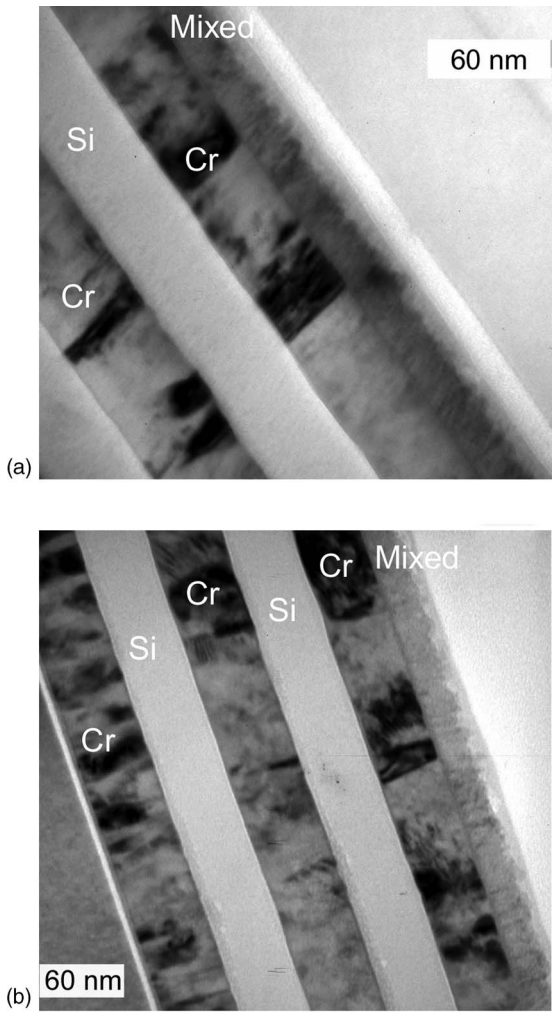

FIG. 4. The XTEM images of samples irradiated by 205 (a) and 410 (b) ions/nm^2. From right to left glue, remaining of Si1+mixed region, remaining Cr1, Si2, Cr2, etc.

by fluences of 205 [Fig. 4(a)]and 410 [Fig. 4(b)] ions/nm^2, respectively. Clearly in both cases the transition between the mixed region and pure Cr is abrupt in good agreement with the AES depth profiling studies.

It is clear that the concentration distribution produced by the Ga^+ irradiation is far from being an error function, thus the mixing behavior of the Ga^+ irradiation basically different from the usual ion mixing process. Now we will see what the predictions of the ballistic models are.

B. SRIM simulation

The penetration depth of the Ga can be estimated by the help SRIM code.[17] The projected ranges of 30 keV Ga^+ ions (angle of incidence with respect of the surface normal is 5°) are 11±6 and 28±10 nm in pure Cr and Si, respectively. One of the consequences of this large difference of the projected ranges in our case is that the Ga range is not a single Gaussian type of curve but rather a curve with two maxima; the second maximum is in the Cr layer. With the decrease (irradiation with higher fluence) of the thickness of Si layer the second maximum is getting larger than the first one. This also means, however, that according to this simulation con-

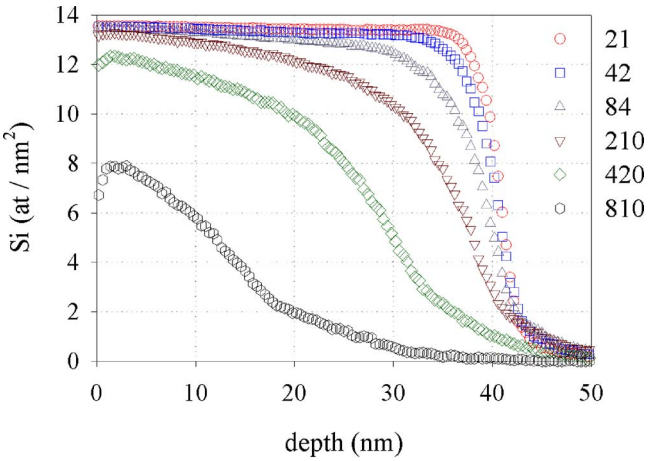

FIG. 5. (Color online) The simulated (TRIDYN) (Ref. 18) concentration distribution curves for the given fluences (ions/nm^2).

siderable energy is deposited in the interface region, which might produce strong ion mixing. In this respect this calculation supports our experimental findings. Though the SRIM simulation is considered, as reliable tool to give the projected range of the ions it tells nothing on the actual damage which is produced by extended ion irradiation.

C. TRIDYN simulation

We have applied TRIDYN simulation of Moller *et al.*[18] to simulate the damage caused by the Ga^+ ion irradiation. [18] The simulation was carried out for the experimental conditions and the input parameters given earlier. The depth distributions of the Si provided by the TRIDYN simulation are shown in Fig. 5. The simulation clearly shows that considerable damage is introduced by the Ga^+ irradiation. The simulated concentration distribution profiles are different from the expected Gaussian distribution, and unfortunately they are different from the measured curves as well. Thus we conclude that the TRIDYN code cannot describe the phenomenon. It also follows that simple ballistic processes cannot explain this mixing process.

D. Qualitative description of the ion mixing process

The Ga^+ irradiation induce mixing is concentrated in the middle stronger mixed region; only this region changes with increasing fluence. We have shown that the stronger mixed region is joined to the underlying pure Cr layer with an abrupt transition independently of the fluence applied. Its connection to the free surface also seems to be independent to the fluence until the strongly mixed region reaches the surface.

Thus to follow the development of the ion mixing as a function of the fluence we should only consider the stronger mixed region. The stronger mixed region can be easily recognized (except for fluence of 25 ions/nm^2) in Fig. 2(a) as the linear part of the Si surface density versus depth curve. Two parameters of this part of the curves have been determined as the thickness and the slope. The data determined are summarized in Table II.

TABLE II. The thickness (nm) and slope of the strongly mixed region as a function of the Ga^+ irradiation.

Irradiation (ions/nm^2)	Thickness (nm)	Slope
51	2.5	−0.66
205	15.2	−0.17
410	24.2	−0.055
820	30	−0.018

At the lowest fluence (25 ions/nm^2) only broadening occurs, but the middle, stronger mixed region cannot be recognized. It should be noted, however, that the shape of the concentration distribution is already not an error function type (the ballistic mixing does not describe it) and the abrupt transition to the underlying layer is present. Applying double fluence (51 ions/nm^2) the middle region can easily be recognized. With increasing fluence the slope of the middle region decreases. It means that with increasing fluence a more and more homogeneous (along the depth) layer is produced. The process can be depicted as the growth of the mixed region into the Si layer, which means the transport of the Cr atoms across the interface.

A somewhat new process starts, when the pure Si is sputtered away from the surface. At this point there is a homogeneously mixed region on the surface of the sample, which is joined to the underlying matrix with a sharp interface. Further sputtering decreases the Si content (the Si source is no more present), but the sharp interface prevail.

The final configuration is a strongly mixed region on the surface of the pure Cr and the two regions are separated by an abrupt transition. This way by varying the fluence we might have variously mixed Si/Cr layer on the surface of a pure Cr and the interface between the two regions is abrupt.

The most unusual is the sharp interface between the strongly mixed region and the pure Cr. We speculate that this always-sharp interface might be explained by strongly asymmetric mixing. If only the Cr can enter into the Si layer, but the Si cannot enter to the Cr layer we get a sharp interface. In this case the number of Cr atoms entered to the Si layer should simply depend on the fluence.

From the true depth profile we can easily determine the number of Cr atoms entered to the Si layer. In Fig. 6 we show the derived data. There is a linear relationship between

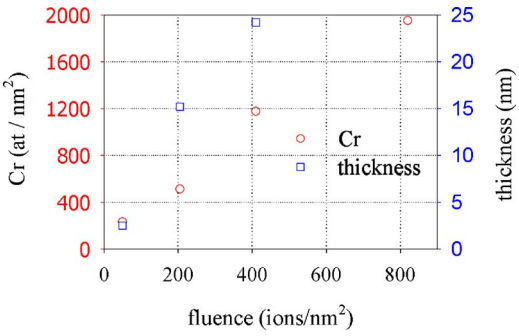

FIG. 6. (Color online) The number of Cr transported into the Si layer through unique area (nm^2) and the thickness of the strongly mixed layer as a function of the fluence.

the number of Cr atoms entered into the Si layer and the fluence; about 2.6 Cr atoms enter to the Si layer per one Ga^+ ion. Figure 6 also shows the thickness values as a function of the fluence, which can be also approximated by a linear relationship. As we have only three points of this curve we do not discuss this dependence in detail.

Is it reasonable to assume asymmetric mixing? We are not aware if anybody assumed such process at medium energy ion mixing. On the other hand, recently we have reported on asymmetric ion mixing in case Pt/Ti bilayer.[28] Two bilayers were made: Pt/Ti and Ti/Pt. These structures were bombarded by Ar^+(1 keV/82°). Deep Pt and no Ti penetrations were found when the Pt and Ti were on the top, respectively. The phenomenon was explained by the large mass anisotropy. On the other hand, we observed similar asymmetric mixing in case of the mass isotropic Cr/Ti system.[29] The driving force in this case has not been identified yet. These findings support that asymmetric mixing was assumed.

V. CONCLUSIONS

Amorphous Si (41 nm)/polycrystalline Cr (46 nm) layered structure was irradiated by Ga^+ ions (energy 30 keV, angle of incidence 5°, with respect the surface normal) applying fluences of 25, 51, 205, 410, and 820 ions/nm^2. The irradiated samples were studied by AES depth profiling, cross-sectional transmission electron microscopy, and atomic force microscopy. The free surface of the sample gets smoother due to the Ga^+ irradiation. AES depth profiling, however, reveals ion mixing between the Si and Cr. The shape of concentration distribution is found to be unusual. Around the original position of the interface there is a stronger (than in the other places) mixed region. The thickness of this region changes with the Ga^+ ion fluence. On the other hand, the interface between the mixed region and the pure Cr is extremely sharp independently from the fluence, which has also been proved by cross-sectional transmission electron microscopy. This behavior is strongly different from the expectation based on high energy ion mixing experiments. Similarly TRIM simulation failed to reproduce the concentration distribution formed. Assuming asymmetric ion mixing (Cr can enter the Si layer but the Si cannot enter the Cr layer) the experimental findings can qualitatively be explained.

ACKNOWLEDGMENTS

The help of the NKFP Project No. 3A/071/2004 and Slovenian-Hungarian TeT of SLO 07/05 are acknowledged. The authors are grateful to A. Jakab for the preparation of the samples for XTEM studies.

[1] MRS Proceedings Vol. 157, edited by J. A. Knapp, P. Borgesen, and R. A. Zuhr, 1989, Part III.
[2] W. Bolse, Mater. Sci. Eng., R **12**, 53 (1994).
[3] M. Menyhard and P. Süle, Surf. Interface Anal. **39**, 487 (2007).
[4] L. Bischoff, Ultramicroscopy **103**, 59 (2005).
[5] D. McGrouther, J. N. Chapman, and F. W. M. Vanhelmont, J. Appl. Phys. **95**, 7772 (2004).
[6] C. Akhmadaliev, B. Schmidt, and L. Bischoff, Appl. Phys. Lett. **89**, 223129 (2006).
[7] J. C. Gonzalez, M. I. N. da Silva, D. P. Griffis, and P. E. Russell, J. Vac. Sci. Technol. B **20**, 2700 (2002).
[8] G. C. Gazzadi, E. Angeli, P. Facci, and S. Frabboni, Appl. Phys. Lett. **89**, 173112 (2006).
[9] L. Bischoff, J. Teichert, and V. Heera, Appl. Surf. Sci. **184**, 372 (2001).
[10] C.-M. Park, J. A. Bain, T. W. Clinton, P. A. A. van der Heijden, and T. J. Klemmer, Appl. Phys. Lett. **84**, 3331 (2004).
[11] W. Boxleitner, G. Hobler, V. Kluppel, and H. Cerva, Nucl. Instrum. Methods Phys. Res. B **175–177**, 102 (2001).
[12] A. Barna, G. Radnóczi, and B. Pécz, in *Handbook for Microscopy*, edited by S. Amelickx, D. Van Dyck, and J. van Tendeloo (VCH Verlaggesellschaft mbH, Weinheim, Germany, 1997), Vol. 3, Part II, Chap. 3, pp. 751–801.
[13] A. Barna and M. Menyhard, Phys. Status Solidi A **145**, 263 (1994).
[14] *Handbook of Auger Electron Spectroscopy*, 3rd ed., edited by K. D. Childs, B. A. Carlson, L. A. LaVanier, J. F. Moulder, D. F. Paul, W. F. Stickle, and D. G. Watson (Physical Electronics, Inc., Eden Prairie, MN, 1995).
[15] L. Kotis, M. Menyhard, L. Toth, A. Zalar, and P. Panjan, Vacuum (in press).
[16] P. Sigmund, *Sputtering by Particle Bombardment I Top. Appl. Phys.*, 47th ed., edited by R. Behrisch (Spinger, Berlin, 1981).
[17] J. F. Ziegler, Transport Range of Ions in Matter. Software freely available from www.srim.org.
[18] W. Möller and M. Posselt, TRIDYN_FZR, FZR-317, Forschungzentrum Rossendorf, 01314 Dresden, Germany.
[19] S. Hofmann, in *Practical Surface Analysis, Auger and X-ray Photoelectron Spectroscopy*, 2nd ed., edited by D. Briggs and M. P. Seah (Wiley, Chichester, 1990), Vol. 1, pp. 143–200.
[20] M. Menyhard, Micron **30**, 255 (1999).
[21] A. Barna, B. Pécz, and M. Menyhard, Micron **30**, 267 (1999).
[22] Z. Csahok, Z. Farkas, M. Menyhard, G. Gergely, and Cs. S. Daroczi, Surf. Sci. Lett. **364**, L600 (1996).
[23] A. Zalar, Thin Solid Films **124**, 223 (1985).
[24] D. P. Adams, T. M. Mayer, M. J. Vasile, and K. Archuleta, Appl. Surf. Sci. **252**, 2432 (2006).
[25] S. M. Rossnagel, R. S. Robinson, and H. R. Kaufman, Surf. Sci. **123**, 89 (1982).
[26] S. Tanuma, C. J. Powell, and D. R. Penn, Surf. Interface Anal. **21**, 165 (1994).
[27] M. Menyhard, Surf. Interface Anal. **26**, 1001 (1998).
[28] P. Süle, M. Menyhard, L. Kotis, J. Labar, and W. F. Egelhoff, Jr., J. Appl. Phys. **101**, 043502 (2007).
[29] M. Menyhard, P. Süle, L. Kotis, and W. F. Egelhoff, Jr. (unpublished).